An ultrasound-assisted photocatalytic treatment to remove an herbicidal pollutant from wastewaters

Schieppati D.[a,b], Galli F.[a,*], Peyot M.L.[c], Yargeau V.[c], Bianchi C.L.[a], Boffito D.C[b]

[a]*Dipartimento di Chimica, Universitá degli Studi di Milano, via Golgi 19, 20133, Milano, Italia*
[b]*Department of Chemical Engineering, Polytechnique Montréal, C.P. 6079, Succ. CV Montréal, H3C 3A7, Québec, Canada*
[c]*Department of Chemical Engineering, McGill University, 3610 University St., Montréal, H3A 2B2, Québec, Canada*

Abstract

Pollutants of emerging concern contaminate surface and ground water. Advanced oxidation processes treat these molecules and degrade them into smaller compounds or mineralization products. However, little information on coupled advanced oxidation techniques and on the degradation pathways of these pollutants is available to identify possible ecotoxic subproducts. In the present work, we investigate the ultrasound assisted photocatalytic degradation pathway of the herbicide Isoproturon. We worked in batch mode in a thermostatic glass reactor. We compared the activity of nanometric TiO_2 P25 with that of Kronos 1077, a micrometric TiO_2. We discuss the individual, additive and synergistic degradation action of photolysis, sonolysis, sonophotolysis, and sonophotocatalysis by varying catalyst loading and/or ultrasound power for the last three techniques. With $0.1\,g\,L^{-1}$ catalyst, photocatalysis and sonophotopcatalysis completely degrade Isoproturon within 240 min and 60 min, respectively ($> 99\,\%$ conversion). Sonophotocatalysis breaks Isoproturon down into smaller molecules than photocatalysis alone.

Keywords: Isoproturon, sonophotodegradation, wastewater treatment, micrometric catalyst, degradation pathway

1. Introduction

The agricultural industry plays a fundamental role in the development and growth of a country. The huge increase of inhabitants elicited the mass cultivation development. Agriculture has now reached such an extent that the use of pesticides (herbicides, fungicides and insecticides) is essential to guarantee the survival of the humankind. Chemicals are classified by their mode of action (MOA), which describes either functional or anatomical changes within cells resulting from the exposure of an organism to that substance. The mode of action represents the level of complexity between molecular mechanisms and physiological outcomes. Modern pesticides act on a specific nuclear receptor or enzyme with a single MOA with few side effects for humans, animals and plants health [1]. However, the use of pesticides with multiple MOA that act on many cell signaling pathways is still in effect at the present day and they pose a serious threat even when applied in tiny amounts.

*Corresponding author
Email address: federico.galli@unimi.it (Galli F.)

The EU Water Framework Directive on Environmental Quality Standards 2008/105/EC announced in Annex X a list of 33 priority substances, which includes metals, pesticides, phthalates, polycyclic aromatic hydrocarbons and endocrine disruptors. Notably, 11 plant protection products are subject to phasing out within an appropriate timetable not exceeding 20 years [2]. While the occurrence and effects of metals, bacteria, hydrocarbons and other ions like nitrates and ammonia in water are extensively described, data on pesticides, pharmaceuticals and phthalates are seldom available. Specifically, herbicides are more water soluble, polar and thermally stable than other contaminants. They have harmful effects on soil, flora and fauna, surface and ground water, which may eventually enter the human being and livestock's food chain [3].

Contaminants enter water bodies in a number of ways, including industrial and municipal discharge, runoff, spills and deposition of airborne pollutants. Most often, waterways are being polluted by agricultural waste containing toxic compounds that cannot be broken down by natural processes.

There is a direct correlation between water pollution and the agricultural practices of the surrounding area [4]. Groundwater pollution is rather persistent and the degradation rate in soil is slow. The concentration of organic pollutants in water and soil depends on the presence of microorganisms, whose activity, in turn, is affected by pH, temperature, moisture and nutrient content. This creates a spatial variability in the degradation rate of pollutants.

The lack of knowledge of the impact on both human health and environment upon long and short-term exposure is one of the main issues of emerging pollutants [5]. Emerging pollutants are new products or chemicals without a regulatory status and whose long-term effects on environment and human health are unknown.

It is of utmost importance to dispose off wastewaters in a proper manner as well as to keep the concentration of chemicals in the effluent stream to a certain minimum level in order to comply with the environmental laws, which are becoming more stringent nowadays. The limit concentration of chemicals allowed by law in drinking water is generally $10\,\mu g\,L^{-1}$ and, for most of pesticides and pharmaceuticals, lower than $0.5\,\mu g\,L^{-1}$ [2].

Isoproturon (IPU) is a phenylurea herbicide widely used for crop protection because of its moderate persistence and relatively low adsorption. On average, the environmental half life of IPU (DT_{50}) is 30 days [6]. However, it has become an occasional water contaminant with proven sub-acute toxicity on rats [7] as well as endocrine disruptor capability on humans [8]. It promotes tumor growth and accounts for other ailments related to the reproductive system [9]. Actually, the 20 % to 40 % by weight of the herbicide drizzled on field remains unaffected and the permitted IPU guideline value in water is not respected [10].

TiO_2 photocatalysis has recently emerged as a green approach to degrade water pollutants. Because of characteristics such as stability, availability, and cost, titanium dioxide (TiO_2) is the foremost exploited photocatalytic material in every field of application [11]. Degussa P25 (TiO_2) catalyst features great performance in aqueous [12, 13] and air environment [14]. However, its applications are limited due to its nanometric particle size, which poses serious threats when it comes to dermal and pulmonary exposure [15]. Micrometric TiO_2 is a valid alternative to P25 as it presents less health concerns. Notwithstanding TiO_2 based catalysts are efficient in terms of wastewater organic pollutants removal, the formation of toxic by-products is to be taken into account [16]. Moreover, the efficacy of photocatalytic processes depends on the nature and composition of the wastewater to be treated.

Research into more efficient wastewater treatment technologies for the degradation of complex refractory molecules into simpler ones is key to improve water quality [17, 18]. Going towards this direction, coupling ultrasound with photocatalysis creates an Advanced Oxidation Process (AOP)

whereby two combined methods contribute to produce OH radicals. Indeed, acoustic cavitation proved to intensify both physical and chemical processes [19, 20, 21, 22].

When applied to a liquid, ultrasonic waves generate vapour-filled voids via a cyclic succession of expansion and compression phases. Upon collapsing, each cavitation bubble acts as a hotspot by generating micro-jets whose energy increases the temperature and pressure up to 5000 K and 500 atm, respectively [23]. These conditions cause water to split and hydroxyl radicals to form. In this sense, ultrasonic cavitation may intensify the photocatalytic wastewater treatment [24]. Mosleh and Rahimi combined ultrasound (25 kHz) and a copper metal organic framework photocatalyst to degrade abamectin [25] and found that there is a synergistic effect between the two AOPs. Some of the same authors degraded trypan blue and vesuvine with a silver metal organic framework (LED light and 25 kHz ultrasound) [26]. Similarly, Vinoth et al. [27] prepared a TiO_2-NiO nanocomposite active under solar light and coupled it with ultrasound (40 kHz) to degrade methyl orange, obtaining a synergy of 4.8 fold. However, only few works focus on IPU degradation pathway. Identifying the subproducts and intermediates yielded in the degradation pathway is of paramount importance to assess their eco and microtoxicity, and select the safest method of degradation as a consequence. Barbeidou et al. studied the sonophotodegradation of malachite green (9 W UVA and 80 kHz ultrasound) and determined the molecule degradation pathway by GC–MS [28]. As far as we know, no one attempted to understand the synergistic effect of ultrasound and photocatalysis on the degradation pathway of water pollutants.

Here, we investigated the ultrasound assisted photocatalytic degradation pathway of the herbicide Isoproturon (IPU) by means of a 100 % anatase micrometric TiO_2 catalyst, Kronos 1077. Our work is original for several reasons: i) we studied the sonophotodegradation of IPU for the first time with Kronos 1077, ii) we optimized catalyst concentration and varied ultrasound power and we demonstrated that micrometric Kronos 1077 is a valid alternative to nano-sized P25, iii) we employed a less harmful material than P25 iv) we propose the IPU degradation pathway using both ultrasound and photocatalysis coupled with ultrasound.

2. Materials and methods

2.1. Materials

We purchased Isoproturon PESTANAL^{TM} analytical standard from Sigma Aldrich. We employed Kronos 1077 as micrometric TiO_2 catalyst and we compared its performance with Degussa P25 nanometric TiO_2 catalyst. The former is 100 % anatase phase and features an average crystallite size of 110 nm whereas the latter has an anatase/rutile phase composition of 80 % and 20 %, respectively [29]. Both catalysts were in powder form. We purchased water and acetonitrile from Fischer Scientific, HPLC grade, submicron filtered. We assessed the influence of dissolved salts by using tap water from Milan water supply network (from June to July 2018).

2.2. Experimental

We ran photocatalytic and sonolytic tests separately at first and we successively combined the two methods in a single sono-photocatalytic process (Table 1). For all tests we employed a thermostatic glass reactor where tap water flew in the cooling jacket that kept the temperature inside the reactor at 15 °C. We dispersed the catalyst in the reaction medium under mild magnetic stirring, which was maintained for the entire duration of the tests. The duration of photocatalytic tests was 6 h and we sampled 2 mL every 60 min, whereas ultrasound-assisted experiments lasted 3 h and we sampled 2 mL every 30 min.

For photocatalytic tests, we filled the reactor with 100 mL of a 20 ppm IPU solution. We selected the initial concentration of IPU to 20 ppm because of the detection limit of the instrumentation. A UVA HG 500 W quartz with halides lamp from Jelosil irradiated the IPU working solution. We arranged the UVA lamp sideways to the reactor at a distance so that the intensity of the UV radiation was equal to $160\,\mathrm{W\,m^{-2}}$. We tested distilled and tap water IPU solutions to assess how the matrix affects the degradation rate of the molecule. We also varied the concentration of the catalysts ($0.05\,\mathrm{g\,L^{-1}}$, $0.1\,\mathrm{g\,L^{-1}}$, and $0.2\,\mathrm{g\,L^{-1}}$) to evaluate the optimal working concentration for both nanometric and micrometric catalysts. Despite photocatalysis and ultrasonic cavitation follow different reaction mechanisms, we ran tests with a catalyst concentration of $0.1\,\mathrm{g\,L^{-1}}$ as it proved to be the optimal one in the first part of the work.

For ultrasonic tests, we filled the reactor with 100 mL of a 20 ppm distilled water IPU synthetic solution. We positioned the ultrasonic processor on top of the reactor and we plunged the US probe 1 cm into the reaction liquid so that it did not touch the glass wall of the reactor. The ultrasonic processor was a VibraCell VCX 500 (Sonics and Materials) working at a nominal power of 50 W and a fixed frequency of 20 kHz. The tip is made of a titanium alloy (Ti-6Al-4V) and its diameter is 13 mm. The probe length is 136 mm. We ran tests at $15\,\mathrm{W\,cm^{-2}}$, $25\,\mathrm{W\,cm^{-2}}$, and $50\,\mathrm{W\,cm^{-2}}$.

Table 1: Summary of the experimental tests

Water type	UV power ($\mathrm{W\,m^{-2}}$)	US power ($\mathrm{W\,cm^{-2}}$)	Catalyst	Catalyst concentration ($\mathrm{g\,L^{-1}}$)
Distilled	160	-	-	-
Tap	160	-	-	-
Distilled	160	-	Kronos 1077	0.05
Distilled	160	-	Kronos 1077	0.1
Distilled	160	-	Kronos 1077	0.2
Tap	160	-	Kronos 1077	0.05
Tap	160	-	Kronos 1077	0.1
Tap	160	-	Kronos 1077	0.2
Distilled	160	-	P25	0.05
Distilled	160	-	P25	0.1
Distilled	160	-	P25	0.2
Tap	160	-	P25	0.05
Tap	160	-	P25	0.1
Tap	160	-	P25	0.2
Distilled	-	15	-	-
Distilled	-	50	-	-
Distilled	160	50	-	-
Distilled	160	25	Kronos 1077	0.1
Distilled	160	25	P25	0.1
Distilled	160	50	Kronos 1077	0.1
Distilled	160	50	P25	0.1

2.3. Analytical Methods

We monitored the degradation of IPU via HPLC-UV and a HPLC-MS identified by–products. The HPLC-UV apparatus uses a Microsorb MV 100–5 C18 250 mm x 4.6 mm column from Agilent Technologies and UV detector. We injected 20 µL of sample and we worked in isocratic mode at 0.5 mL min^{-1} with a mobile phase composition of H_2O:ACN 1:1. We kept the column at 30 °C. The detection wavelength for IPU was 240 nm. We repeated each analysis twice. HPLC–UV provided with Varian ProStar 6.41 workstation quantitatively monitored only the conversion of IPU, as no by–product appeared nearby its peak, which remained sharp and well outlined. We analyzed IPU and its degradation products by liquid chromatography at atmospheric pressure and heated electrospray ionization (ESI) tandem mass spectrometry. The system consists of an Accela 600 HPLC coupled to an Orbitrap LTQ XL mass spectrometer from Thermo Scientific. For the chromatographic separation we used a HPLC Zorbax Eclipse Plus C18 guard column (5 mm x 4.6 mm ID; 5 µm) followed by an analytical column Zorbax Eclipse Plus C18 (250 mm x 4.6 mm ID; 5 µm), both from Agilent Technologies. We injected 20 µL of sample upon prior dilution 1:5 in LC-MS grade water and we followed the same chromatographic separation conditions and analysis repetitions indicated for the HPLC-UV method.

A Thermo Scientific LTQ XL mass spectrometer scanned IPU samples by Fourier-Transform (FT) and ion trap (IT–MS) in positive mode. The spectrometer accommodates a high resolution Orbitrap detector (MS), which is in tandem with the HPLC system. The spectrometer also lodges a pneumatic assisted heated ESI source. We set the heater at 300 °C and the temperature of the capillary was 375 °C.

We optimized the instrument detection parameters by direct infusion of 2 ppm IPU analytical standard at 10 µL min^{-1}. For source optimization we used helium as collision gas and nitrogen as auxiliary, sweep and sheath gas for focusing gases in the source. The FT detector acquired information in full scan mode from 50 m/z to 600 m/z at 60 000 high resolution with a mass accuracy tolerance of 5 ppm. We set the ion trap with 22 specific transitions by using a collision induced dissociation (CID) of 45 % normalized collision energy (NCE) to ensure the generation of product ions on the MS2 spectra for the identification of the selected precursor ions. A Thermo Xcalibur software (Thermo Scientific, Waltham, MA, USA) and the open-source software MZmine 2 processed, visualized, and profiled data analysis.

3. Results and discussion

3.1. Photolysis and photocatalysis

Photolysis converted 18 % and 10 % of IPU in 6 h in distilled and tap water, respectively (Figure 1).

We obtained a half-life time of 23 h in distilled water, assuming a first order kinetic (kinetic constant of 0.0005 min^{-1}, R^2 = 0.98). Dureja et al. [30], report a IPU half-life time of 5 h and 30 h under UV and visible irradiation, respectively. (wavelength from 254 nm to 300 nm, 125 W). However, Sanches et al. [31] photolized IPU with a low pressure Hg lamp emitting at 254 nm and observed an IPU first order degradation kinetic constant of 0.0006 min^{-1}, which agrees with our results. Photolysis of organic compounds is generally less active in deionized water [32] than in aqueous solution containing salts. For instance, 1 mg L^{-1} of 2,4-Dinitrotoluene photolizes with an half-life of 1 h in seawater and in 4 h in distilled water [33]. We hypothesize that the complex matrix of Milano tap water contains molecules (such as other pharmaceuticals or small amount of organics) that absorb UV radiation and compete to IPU degradation, leading to lower IPU photoconversion.

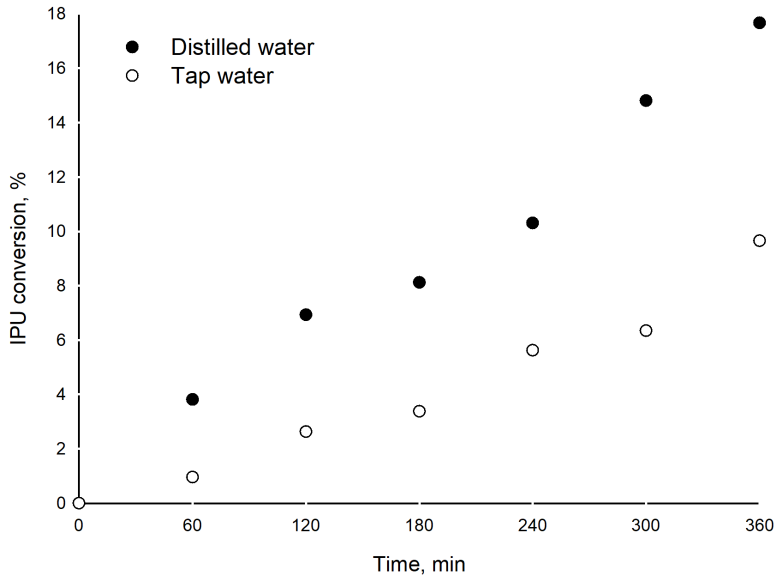

Figure 1: Photolytic degradation of IPU in Milan tap and distilled water. Maximum error is ±3% considering two repetitions and instrument resolution.

In fact, Azzelino et al. [34] report an average chemical oxygen demand and biological oxygen demand in Lombardy waters of $7.94\,\mathrm{mg\,L^{-1}}$ and $2.54\,\mathrm{mg\,L^{-1}}$, respectively. Therefore, scientists should tune the experimental parameters for each water matrix and pollutants. We then evaluated how the concentration of the catalyst charged into the reactor affects the final conversion of IPU, either in distilled or tap water (Figure 2).

With a catalyst concentration of $0.1\,\mathrm{g\,L^{-1}}$ and $0.2\,\mathrm{g\,L^{-1}}$ we achieved complete IPU conversion in 6 h. We chose $0.1\,\mathrm{g\,L^{-1}}$ as optimal concentration to pursue further tests as it provides the same results as a concentration of $0.2\,\mathrm{g\,L^{-1}}$. Moreover, $0.1\,\mathrm{g\,L^{-1}}$ is the standard catalyst concentration loaded within the reactor for most photochemical reactions as it does not screen the UV radiation excessively [35].

In distilled water, Kronos and P25 behave similarly (Figure 2a and Figure 2b). In fact, they reach the same final conversion in 6 h at any catalyst concentration. In tap water, experiments show comparable kinetic rates for both Kronos ($0.0049\,\mathrm{min^{-1}}$ at $0.05\,\mathrm{g\,L^{-1}}$ and $0.0088\,\mathrm{min^{-1}}$ at $0.1\,\mathrm{g\,L^{-1}}$) and P25 ($0.0058\,\mathrm{min^{-1}}$ at $0.05\,\mathrm{g\,L^{-1}}$ and $0.0176\,\mathrm{min^{-1}}$ at $0.1\,\mathrm{g\,L^{-1}}$) at all catalyst concentrations but $0.2\,\mathrm{g\,L^{-1}}$. In this case, P25 (kinetic constant of $0.025\,\mathrm{min^{-1}}$) exhibits a better performance than Kronos (kinetic constant of $0.015\,\mathrm{min^{-1}}$) (Figure 2c and Figure 2d).

Photodegradation rates depend on salt concentration, pH, COD of water and size of catalyst aggregates [36]. Therefore, we executed all the remaining tests in distilled water to assess the fragmentation pathway in different processes in an ideal case, i.e. with no matrix effect.

3.2. Sonolysis

We investigated sonolysis at an ultrasound power of $15\,\mathrm{W\,cm^{-2}}$ and $50\,\mathrm{W\,cm^{-2}}$.

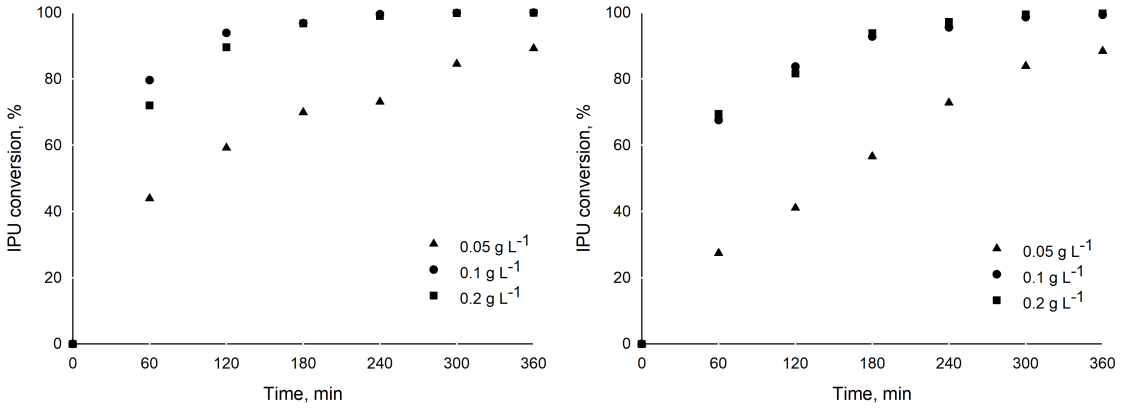

(a) Kronos 1077, distilled water

(b) P25, distilled water

(c) Kronos 1077, tap water

(d) P25, tap water

Figure 2: Photocatalytic degradation of IPU with different catalysts concentration. Maximum error is ±3% considering two repetitions and instrument resolution.

Sonolysis degrades 75 % of IPU in 3 h (Figure 3). It is more effective than UVA photolysis, which converts 9 % of IPU in distilled water in 6 h (Figure 1). However, HPLC-UV revealed several by-products. Sonication alone is not powerful enough to ensure the complete degradation of IPU, therefore, we merged UVA radiation and ultrasound to intensify the degradation process.

3.3. Sonophocatalysis

We worked at an ultrasound power of 25 W cm^{-2} and 50 W cm^{-2}.

Generally, for the sonolytic degradation, the higher the ultrasound power, the greater the IPU sonodegradation [37], and our results confirm this. Sonophotolysis degrades 36 % of IPU in 3 h at 50 W cm^{-2} (Figure 3). We observe that the addition of ultrasonic cavitation to photolysis promotes IPU degradation compared to the photolytic process (Figure 1,and 3). Furthermore, the final conversion reached with sonolysis (Figure 3) is two times superior than that obtained with

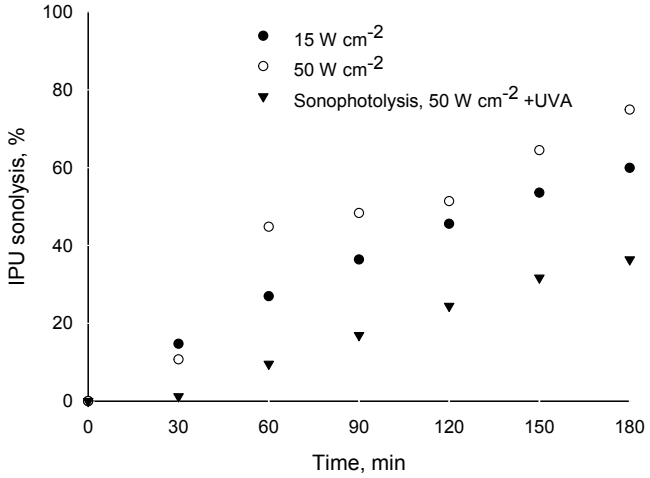

Figure 3: Sonolytic degradation of IPU in distilled water at $15\,\mathrm{W\,cm^{-2}}$ and $50\,\mathrm{W\,cm^{-2}}$ and sonophotolytic degradation of IPU at $50\,\mathrm{W\,cm^{-2}}$. Maximum error is $\pm 3\%$ considering two repetitions and instrument resolution.

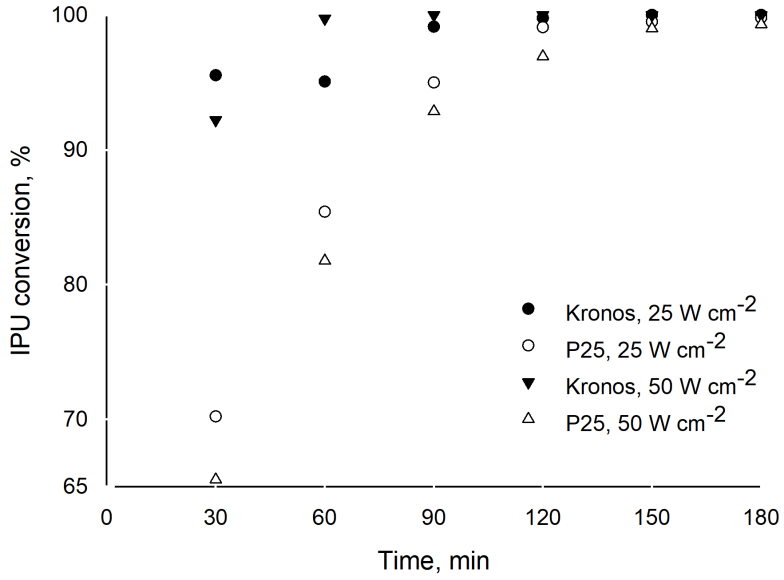

Figure 4: Sonophotocatalytic degradation of IPU in distilled water. Catalyst concentration is $0.1\,\mathrm{g\,L^{-1}}$. Maximum error is $\pm 3\%$ considering two repetitions and instrument resolution.

sonophotolysis (Figure 4). This opposes the accepted idea that photolysis and sonolysis effects are additive or even synergistic [38]. Indeed, Peller et al. proved that coupling sonolysis and photolysis does not change the degradation lifetime of 2,4-Dichlorophenol [39]. Park et al. demonstrated

that the energy ratio between UV and US should be tuned to maximize sonophotodegradation of trihalomethanes [40]. For these components, the photolysis has a predominant role due to the liable C−Br bonds present in the molecules studied, thus the optimum ratio resulted US : UV = 1 : 3 and US : UV = 0 : 4. We did not aim at optimizing such ratio, but we speculate that IPU, not having liable bonds, may require more energy than the one provided by just UV to be degraded. However, in our case coupling ultrasound and photolysis seems even detrimental. The reasons behind this behavior remains to be explained with further experiments.

Sonophotocatalysis in distilled water converted 100 % of IPU in 3 h with both catalysts and at both ultrasound power tested (Figure 4). Photocatalysis with Kronos and P25 at 25 W cm^{-2} and 50 W cm^{-2} achieved 100 % conversion of IPU in 3 h.

Specifically, Kronos converts more than 99 % of IPU in 60 min at 50 W cm^{-2} and in 90 min at 25 W cm^{-2}. P25 converts 100 % of IPU in 120 min at 25 W cm^{-2} and 50 W cm^{-2}.

3.4. By-products analysis

HPLC-UV by–products' peaks were broad and not sharp. This indicated that by-products featured similar polarity and, as a result, they exited the column with almost the same retention time.

LC-MS/MS spectra identified two main types of by-products for both the photocatalytic and sonophotocatalytic degradation processes (see Fig S1 and S2 in the Supporting Information).

The first class forms upon the oxidation of IPU by highly reactive hydroxyl radicals, which is ascribable to the general reactivity of TiO_2 in aqueous environment. The substitution by $^{\bullet}$OH radicals takes place on the benzene ring (structures 221A, 223D, and 239A), the isopropylic group (structures 209 A/B, 221C, and 223A/B), and on the dimethylamine group (structures 221B and 223C/E). MS also revealed multiple hydroxylation on the aromatic ring and on the isopropylic group (structures 225B/A, 237, 239A/B/C, 255A/B/C, 268, and 284).

The second class makes up derivatives in which entire substituents, like methyl or isopropyl, are replaced by an hydroxyl radical. Such reactions take place at various position on the IPU molecule and on by–products themselves (structures 167 and 181).

IPU also undergoes simple N–demethylation or dehydrogenation of the isopropyl group (structures 191, 193, 205, and 221A).

As far as photocatalysis and sonophotocatalysis with Kronos are concerned, LC-MS/MS analyses pointed out two different IPU fragmentation patterns.

Photocatalysis elicited the formation of higher molecular weight by-products in the first part of the reaction (from 30 min to 90 min), originating from the oxidation and recombination of high molecular weight fragments (from 209 m/z to 296 m/z, Table 2).

On the contrary, sonophotocatalysis fragmented the pesticide into molecules with a lower molecular weight than that of IPU (from 167 m/z to 205 m/z) in the same range time mentioned hereinabove (Table 3).

Table 2 summarizes the structures of the by–products identified after the degradation of IPU by UVA light.

During photocatalytic treatment, many intermediates form after 1 h of reaction (see Table S1 in the Supporting Information material for the raw data). After 2 h, such intermediates undergo oxidation to form heavier by–products (Figure 5). Throughout the reaction, we identified 21 by–products, many of which were already reported [41, 42]. In particular, Amorisco et al. [43] describe how by–product 225 originates from structure 209A. However, according to our analysis, by–product 225B might derive also from structure 223A as the concavity of the curve for structure 225B changes

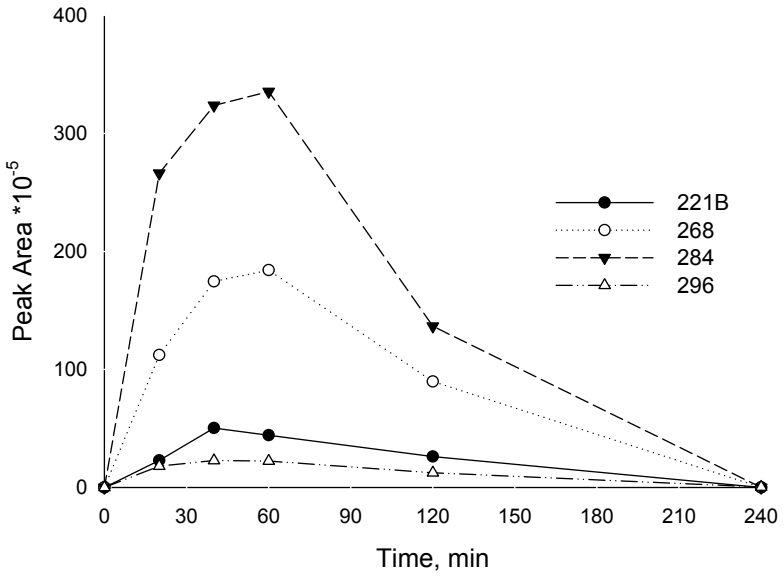

Figure 5: Evolution trend of higher molecular weight structures from intermediate 221B during photocatalytic treatment.

when the curve for structure 223A reaches its maximum at 30 min, as in the case of structure 209A (Figure 7).

Molecules 268, 284, and 296 have never been reported before (Table 2). We successfully identified 268 and 284 by analyzing the MS fragmentations patterns provided by HPLC-MS. For structure 268 we observed fragments corresponding to the loss of the hydroxy group on the aromatic ring and of the carboxylic oxygen on the isopropylic group in para position to the urea group. The MS also reported fragmentation corresponding to the carboxylic acid group bonded to the urea. For structure 284 we observed fragmentation related to the second hydroxy group on the aromatic ring. Molecule 296 structure remains unknown. Therefore, we propose the IPU degradation pathway without considering product 296 (Figure 6).

The sonophotocatalytic degradation mechanism differs from that observed in the photodegradation. In fact, almost all by–products identified originate directly from IPU and few reaction intermediates were observed (see Table S2 in the Supporting Information material for the raw data).

The fact that sonophotocatalysis provokes the generation of lower molecular weight by–products than photocatalysis alone is likely related to the presence of a higher concentration of hydroxyl radicals, which accelerates the oxidation process and promotes fragmentation. Moreover, at the end of the reaction, no byproduct was detected by HPLC-MS (Figure 8). Table 3 reports all the by–products identified after sonophotocatalytic treatment.

Molecules 167, 187, 254, 268, 280, and 296 have never been reported before. We successfully identified 167, 268, but 187, 254, 280, and 296 structures remain unknown (Figure 9). For molecule 268 we observed the same fragmentation pattern as in the case of photocatalytic treatment. For

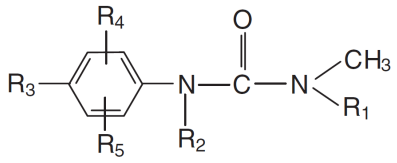

Molecule	R_1	R_2	R_3	R_4	R_5
181	CH_3	H	OH	–	–
191	CH_3	H	$CHCH_2$	–	–
193	H	H	$CH_2(CH_3)_2$	–	–
205	CH_3	H	$CH(CH_2)CH_3$	–	–
209 A	CH_3	H	$CH_2(CH_3)OH$	–	–
209 B	H	H	$C(CH_3)_2OH$ or $CH_2(CH_3)CH_2OH$	–	–
221 A	CH_3	H	$CH(CH_2)CH_3$	OH	–
221 B	C(O)H	H	$CH_2(CH_3)_2$	–	–
223 A	CH_3	H	$CH_2(CH_3)CH_2OH$	–	–
223 C	CH_3OH	H	$CH_2(CH_3)_2$	–	–
223 D	CH_3	H	$CH_2(CH_3)_2$	OH	–
223 E	CH_3	OH	$CH_2(CH_3)_2$	–	–
225 B	CH_3	H	$CH(OH)CH_2OH$	–	–
239 A	CH_3	H	$C(CH_3)_2OH$	OH	–
239 B	CH_3	H	$CH(CH_2OH)_2$ or $C(CH_3)(OH)CH_2OH$	–	–
239 C	CH_3	H	$CH_2(CH_3)_2$	OH	OH
255 A	CH_3	H	$C(CH_3)_2OH$ or $CH_2(CH_3)CH_2OH$	OH	OH
255 B	CH_3	OH	$C(CH_3)_2OH$ or $CH_2(CH_3)CH_2OH$	OH	–
255 C	CH_3	OH	$C(CH_3)_2OH$ or $CH_2(CH_3)CH_2OH$	OH	–
268	C(O)OH	H	$CH(CH_3)C(O)H$	OH	–
284	C(O)OH	H	$CH(CH_3)C(O)H$	OH	OH

Table 2: By–products identified upon photocatalytic treatment.

molecule 167, the HPLC–MS reported fragmentations corresponding to the loss of the isopropyl group in para position to the urea, and corresponding to the hydroxy group on the urea group (specifically, on the nitrogen atom directly bonded to the aromatic ring). All the by-products identified are phenyl ureas, which possess a pharmacological action as anticonvulsant, antimicrobial, antiviral and anti inflammatory agents [44]. Photocatalysis is unable to degrade aryl intermediates in 6 h, yielding a wastewater that may be either as toxic or more toxic than isoproturon-contaminated water. Instead, the sonophotocatalytic process, completely removes phenyl ureas in 3 h.

As reported by Noorimotlagh et al., the wastewater pH affects the degradation process of organic

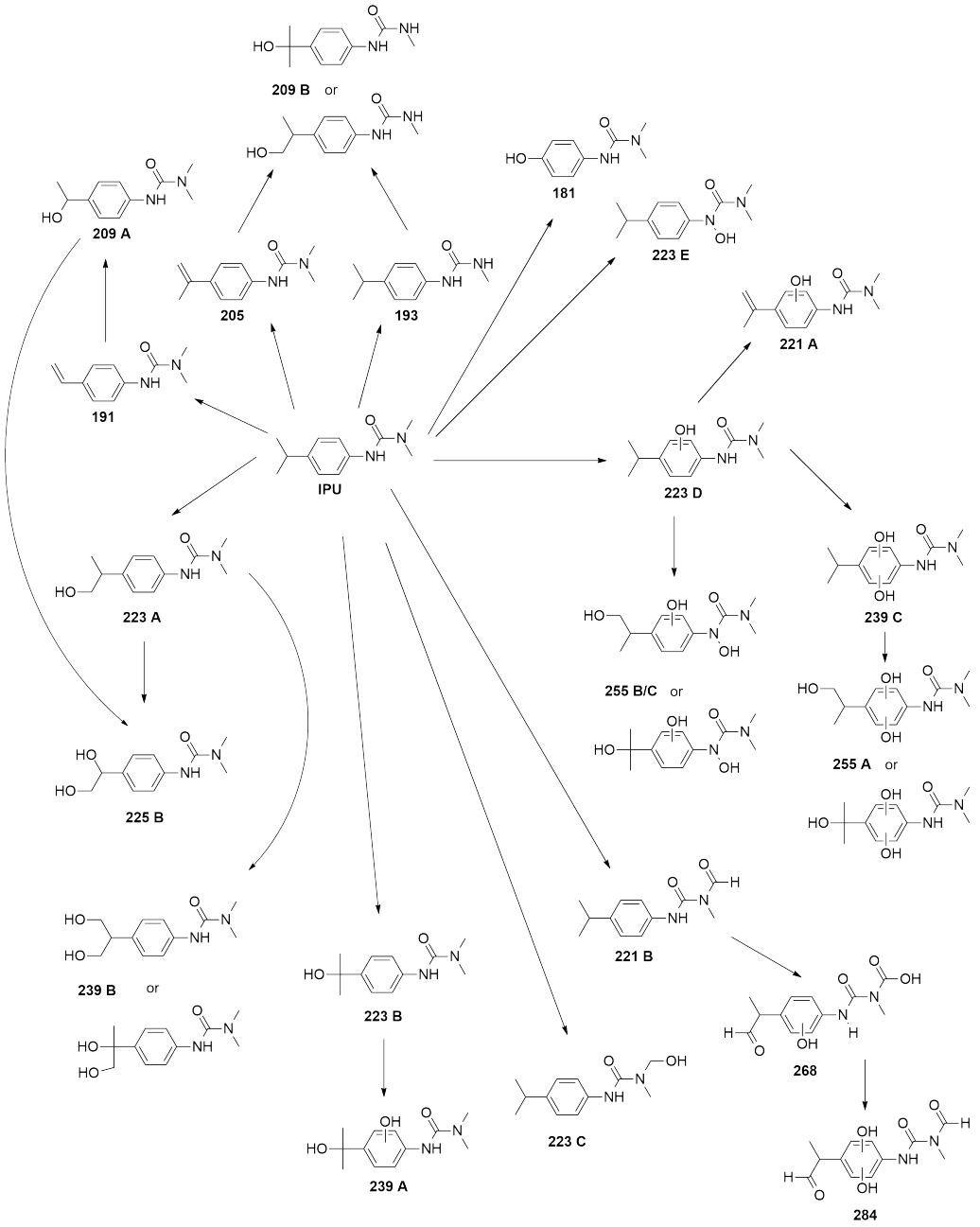

Figure 6: IPU degradation pathway upon photocatalytic treatment.

pollutants [45]. In the present work, we did not modify the pH as the addition of an extra chemical compound would impact on the cost of the treatment in a real industrial plant and would increase

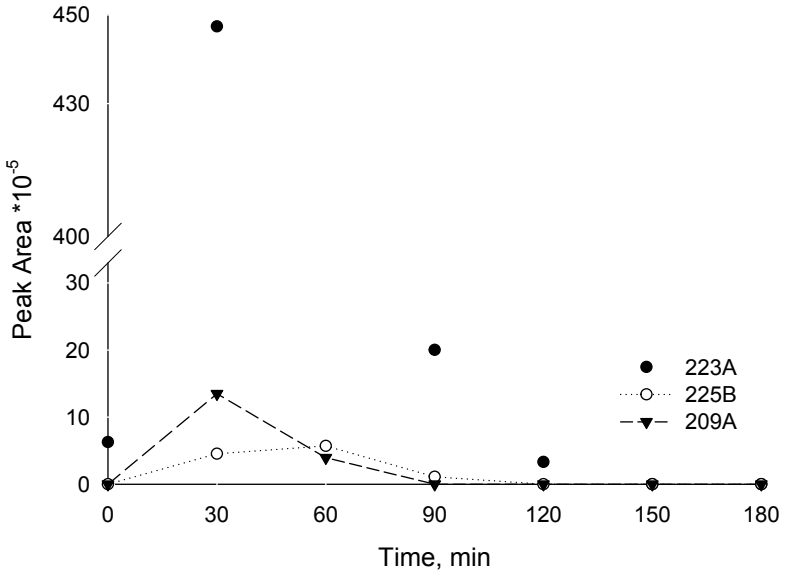

Figure 7: Evolution trend of by–product 225B from 209A and from 223A.

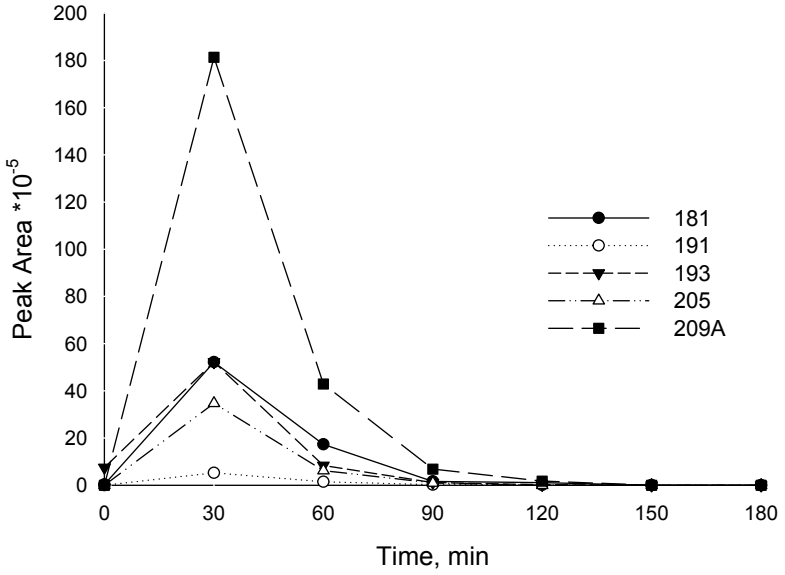

Figure 8: Evolution trend of lower molecular weight structures from IPU during sonophotocatalytic treatment.

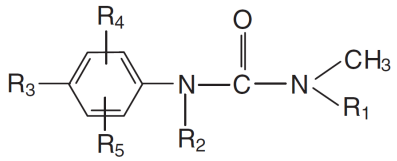

Molecule	R_1	R_2	R_3	R_4	R_5
167	OH	H	H	–	–
181	CH_3	H	OH	–	–
191	CH_3	H	$CHCH_2$	–	–
193	H	H	$CH_2(CH_3)_2$	–	–
205	CH_3	H	$CH(CH_2)CH_3$	–	–
209 A	CH_3	H	$CH_2(CH_3)OH$	–	–
209 B	H	H	$C(CH_3)_2OH$	–	–
			or $CH_2(CH_3)CH_2OH$		
221 A	CH_3	H	$CH(CH_2)CH_3$	OH	–
221 B	C(O)H	H	$CH_2(CH_3)_2$	–	–
221 C	CH_3	H	$CH(CH_3)C(O)H$	–	–
223 A	CH_3	H	$CH_2(CH_3)CH_2OH$	–	–
223 B	CH_3	H	$C(CH_3)_2OH$	–	–
223 C	CH_3OH	H	$CH_2(CH_3)_2$	–	–
223 D	CH_3	H	$CH_2(CH_3)_2$	OH	–
223 E	CH_3	OH	$CH_2(CH_3)_2$	–	–
225 A	CH_3	H	$CH(OH)CH_3$	OH	–
225 B	CH_3	H	$CH(OH)CH_2OH$	–	–
237	CH_3	H	$CH(CH_3)C(O)H$	OH	–
239 A	CH_3	H	$C(CH_3)_2OH$	OH	–
255 A	CH_3	H	$C(CH_3)_2OH$	OH	OH
			or $CH_2(CH_3)CH_2OH$		
255 B	CH_3	OH	$C(CH_3)_2OH$	OH	–
			or $CH_2(CH_3)CH_2OH$		
255 C	CH_3	OH	$C(CH_3)_2OH$	OH	–
			or $CH_2(CH_3)CH_2OH$		
268	C(O)OH	OH	$CH(CH_3)C(O)H$	OH	–

Table 3: By–products identified upon sonophotocatalytic treatment.

the complexity of the matrix to treat.

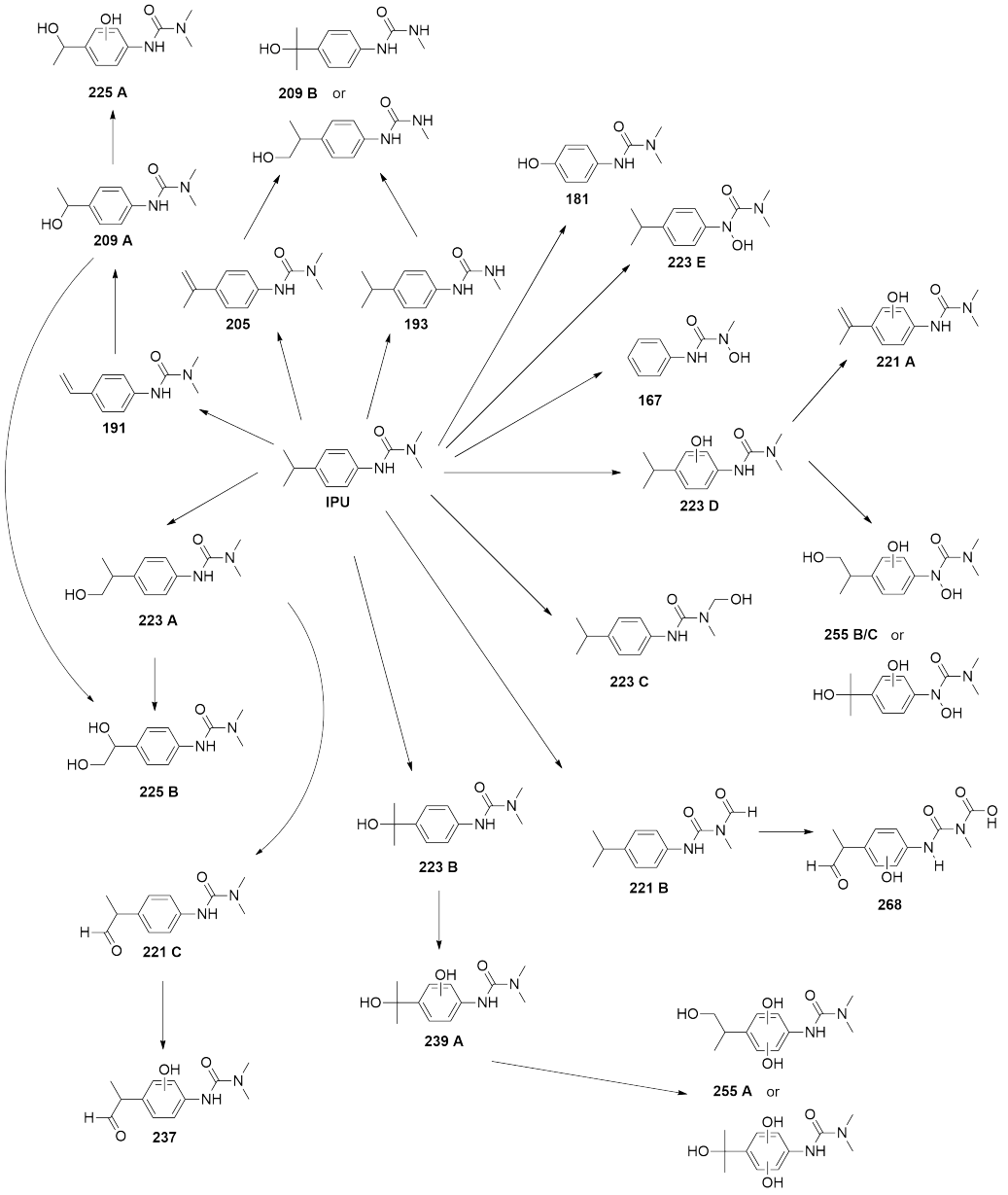

Figure 9: IPU degradation pathway upon sonophotocatalytic treatment.

4. Conclusions

Sonophotocatalysis with an ultrasonic power of 50 W cm^{-2} degrades 100 % of Isoproturon (IPU) in less than 1 h. We demonstrate that Kronos 1077 is a valid photocatalyst to substitute P25, which is nanometric and poses serious health and environmental concerns. Both catalysts were

equally active in the degradation of IPU at a catalyst concentration of $0.1\,\mathrm{g\,L^{-1}}$, whereby complete conversion was achieved in maximum 150 min at both $50\,\mathrm{W\,cm^{-2}}$ and $25\,\mathrm{W\,cm^{-2}}$.

We proposed the degradation pathway of Isoproturon in photocatalytic and sonophotocatalytic processes. We detected 7 by-products that were never reported before, of which 3 were identified. Ultrasound coupled with photocatalysis leads to lower molecular weight byproducts compared to photocatalysis alone. However, coupling ultrasound with UV irradiation in absence of a photocatalyst is detrimental for the degradation of IPU. This result remains to be explained. Further studies will also investigate the stability and reusability of the catalyst and disclose the effect of dissolved salts on Isoproturon degradation pathway.

Acknowledgements

The Authors acknowledge Projet de coopération Québec Italie 2017-2019 (project number: QU17MO09) for granting the mobility of researchers between Canada and Italy. This research was undertaken, in part, thanks to funding from the Canada Research Chairs program.

References

[1] J. Stenersen, Chemical pesticides mode of action and toxicology, CRC press, 2004.

[2] E. Parliament, Directive 2008/105/ec, Off. J. EU (2008).

[3] B. Rashid, T. Husnain, S. Riazuddin, Herbicides and pesticides as potential pollutants: A global problem, in: M. Ashraf, M. Ozturk, M. S. A. Ahmad (Eds.), Plant Adaptation and Phytoremediation, Springer Netherlands, Dordrecht, 2010, pp. 427–447.

[4] S. Rodriguez-Mozaz, M. L. de Alda, D. Barceló, Monitoring of estrogens, pesticides and bisphenol a in natural waters and drinking water treatment plants by solid-phase extraction–liquid chromatography–mass spectrometry, J. Chrom. A 1045 (2004) 85 – 92.

[5] T. Deblonde, C. Cossu-Leguille, P. Hartemann, Emerging pollutants in wastewater: A review of the literature, Int. J. Hygiene Environ. Health 214 (2011) 442 – 448.

[6] A. Walker, M. Jurado-Exposito, G. Bending, V. Smith, Spatial variability in the degradation rate of isoproturon in soil, Environ. Poll. 111 (2001) 407 – 415.

[7] S. Sarkar, S. Chattopadhyay, A. Majumdar, Subacute toxicity of urea herbicide, isoproturon, in male rats, Indian J. Exp. Biol. 33 (1995) 851—856.

[8] F. Orton, I.Lutz, W. Kloasr, E. Routledge, Endocrine disrupting effects of herbicides and pentachlorophenol: In vitro and in vivo evidence, Environ. Sci. & Techn. 43 (2009) 2144–2150.

[9] R. Kramer, R. Baker, Herbicides, Environ. Tech. Human Health 1 24 (2009) 199–204.

[10] M. Younes, H. Galal-Gorchev, Pesticides in drinking water–a case study, Food Chem. Tox. 38 (2000) S87 – S90.

[11] H. Khan, M. Rigamonti, G. Patience, D. Boffito, Spray dried $TiO_{2/}WO_3$ heterostructure for photocatalytic applications with residual activity in the dark, Appl. Catal. B: Environ. 226 (2018) 311–323.

[12] F. Galli, M. Compagnoni, D. Vitali, C. Pirola, C. L. Bianchi, A. Villa, L. Prati, I. Rossetti, CO_2 photoreduction at high pressure to both gas and liquid products over titanium dioxide, Appl. Catal. B: Environ. 200 (2017) 386–391.

[13] M. Pirilä, M. Saouabe, S. Ojala, B. Rathnayake, F. Drault, A. Valtanen, M. Huuhtanen, R. Brahmi, R. L. Keiski, Photocatalytic degradation of organic pollutants in wastewater, Topic. Catal 58 (2015) 1085–1099.

[14] C. L. Bianchi, C. Pirola, F. Galli, G. Cerrato, S. Morandi, V. Capucci, Pigmentary TiO_2: A challenge for its use as photocatalyst in NOx air purification, Chem. Eng. J. 261 (2015) 76–82.

[15] C. M. Sayes, R. Wahi, P. A. Kurian, Y. Liu, J. L. West, K. D. Ausman, D. B. Warheit, V. L. Colvin, Correlating nanoscale titania structure with toxicity: A cytotoxicity and inflammatory response study with human dermal fibroblasts and human lung epithelial cells, Toxicol. Sci. 92 (2006) 174–185.

[16] V. Manilal, A. Haridas, R. Alexander, G. Surender, Photocatalytic treatment of toxic organics in wastewater: Toxicity of photodegradation products, Water Res. 26 (1992) 1035 – 1038.

[17] M. Stucchi, A. Elfiad, M. Rigamonti, H. Khan, D. Boffito, Water treatment: $Mn-TiO_2$ synthesized by ultrasound with increased aromatics adsorption, Ultrason. Sonochem. 44 (2018) 272 – 279.

[18] A. Elfiad, D. Boffito, S. Khemassia, F. Galli, S. Chegrouche, L. Meddour-Boukhobza, Water treatment: $Mn-TiO_2$ synthesized by ultrasound with increased aromatics adsorption, Can. J. Chem. Eng. 96(7) (2018) 1566 – 1575.

[19] D. Boffito, V. Crocellà, C. Pirola, B. Neppolian, G. Cerrato, M. Ashokkumar, C. Bianchi, Ultrasonic enhancement of the acidity, surface area and free fatty acids esterification catalytic activity of sulphated zro2– tio2 systems, J. Catal. 297 (2013) 17 – 26.

[20] P. Louyot, C. Neagoe, F. Galli, C. Pirola, G. S. Patience, D. C. Boffito, Ultrasound-assisted impregnation for high temperature fischer-tropsch catalysts, Ultrason. Sonochem. 48 (2018) 523–531.

[21] D. Boffito, C. Pirola, C. Bianchi, G. Cerrato, S. Morandi, M. Ashokkumar, Sulphated inorganic oxides for methyl esters production: Traditional and ultrasound-assisted techniques, in: R. Luque, A. M. Balu (Eds.), Producing Fuels and Fine Chemicals from Biomass Using Nanomaterials, CRC Press, 2013, pp. 137–162.

[22] A. R. Bagheri, M. Arabi, M. Ghaedi, A. Ostovan, X. Wang, J. Li, L. Chen, Dummy molecularly imprinted polymers based on a green synthesis strategy for magnetic solid-phase extraction of acrylamide in food samples, Talanta 195 (2019) 390 – 400.

[23] T. Y. Wu, N. Guo, C. Y. Teh, J. X. W. Hay, Theory and Fundamentals of Ultrasound, Springer Netherlands, Dordrecht, 2013, pp. 5–12. doi:10.1007/978-94-007-5533-8_2.

[24] N. H. Ince, Ultrasound-assisted advanced oxidation processes for water decontamination, Ultrason. Sonochem. 40 (2018) 97–103.

[25] S. Mosleh, M. R. Rahimi, Intensification of abamectin pesticide degradation using the combination of ultrasonic cavitation and visible-light driven photocatalytic process: Synergistic effect and optimization study, Ultrason. Sonochem. 35 (2017) 449–457.

[26] S. Mosleh, M. Rahimi, M. Ghaedi, K. Dashtian, Sonophotocatalytic degradation of trypan blue and vesuvine dyes in the presence of blue light active photocatalyst of Ag_3PO_4/Bi_2S_3-HKUST-1-MOF: Central composite optimization and synergistic effect study, Ultrason. Sonochem. 32 (2016) 387–397.

[27] R. Vinoth, P. Karthik, K. Devan, B. Neppolian, M. Ashokkumar, TiO_2–NiO p–n nanocomposite with enhanced sonophotocatalytic activity under diffused sunlight, Ultrason. Sonochem. 35 (2017) 655 – 663.

[28] C. Berberidou, I. Poulios, N. Xekoukoulotakis, D. Mantzavinos, Sonolytic, photocatalytic and sonophotocatalytic degradation of malachite green in aqueous solutions, Appl. Catal. B: Environ. 74 (2007) 63–72.

[29] C. Bianchi, C. Pirola, F. Galli, M. Stucchi, S. Morandi, G. Cerrato, V. Capucci, Nano and micro-TiO_2 for the photodegradation of ethanol: experimental data and kinetic modelling, RSC Adv. 5 (2015) 53419–53425.

[30] P. Dureja, S. Walia, K. K. Sharma, Photolysis of isoproturon in aqueous solution, Toxicol. & Environ. Chem. 34 (1991) 65–71.

[31] S. Sanches, M. T. B. Crespo, V. J. Pereira, Drinking water treatment of priority pesticides using low pressure UV photolysis and advanced oxidation processes, Water Res. 44 (2010) 1809–1818.

[32] M. W. Lam, K. Tantuco, S. A. Mabury, Photofate: A new approach in accounting for the contribution of indirect photolysis of pesticides and pharmaceuticals in surface waters, Environ. Sci. & Tech. 37 (2003) 899–907.

[33] O. Mihas, N. Kalogerakis, E. Psillakis, Photolysis of 2,4-dinitrotoluene in various water solutions: effect of dissolved species, J. Hazar. Mat. 146 (2007) 535–539.

[34] A. Azzellino, S. Canobbio, S. Çervigen, V. Marchesi, A. Piana, Disentangling the multiple stressors acting on stream ecosystems to support restoration priorities, Water Sci. & Tech. 72 (2015) 293–302.

[35] G. Cerrato, C. Bianchi, F. Galli, C. Pirola, S. Morandi, V. Capucci, Micro-TiO_2 coated glass surfaces safely abate drugs in surface water, J. Hazar. Mat. (2018).

[36] N. Rioja, S. Zorita, F. J. Peñas, Effect of water matrix on photocatalytic degradation and general kinetic modeling, Appl. Catal. B: Environ. 180 (2016) 330–335.

[37] R. A. Torres-Palma, E. A. Serna-Galvis, Sonolysis, in: S. C. Ameta, R. Ameta (Eds.), Advanced Oxidation Processes for Waste Water Treatment, Academic Press, 2018, pp. 177–213. doi:10.1016/B978-0-12-810499-6.00007-3.

[38] H. C. Yap, Y. L. Pang, S. Lim, A. Z. Abdullah, H. C. Ong, C.-H. Wu, A comprehensive review on state-of-the-art photo-, sono-, and sonophotocatalytic treatments to degrade emerging contaminants, Int. J. Environ. Sci. Tech. (2018).

[39] J. Peller, O. Wiest, P. V. Kamat, Synergy of combining sonolysis and photocatalysis in the degradation and mineralization of chlorinated aromatic compounds, Environ. Sci. & Tech. 37 (2003) 1926–1932.

[40] B. Park, E. Cho, Y. Son, J. Khim, Distribution of electrical energy consumption for the efficient degradation control of THMs mixture in sonophotolytic process, Ultrason. Sonochem. 21 (2014) 1982–1987.

[41] M. López-Munoz, A. Revilla, J. Aguado, Heterogeneous photocatalytic degradation of isoproturon in aqueous solution: Experimental design and intermediate products analysis, Catal. Today 209 (2013) 99 – 107.

[42] I. Losito, A. Amorisco, F. Palmisano, Electro-fenton and photocatalytic oxidation of phenylurea herbicides: An insight by liquid chromatography–electrospray ionization tandem mass spectrometry, Appl. Catal. B: Environ. 79 (2008) 224 – 236.

[43] A. Amorisco, I. Losito, F. Palmisano, P. G. Zambonin, Photocatalytic degradation of the herbicide isoproturon: Characterisation of by-products by liquid chromatography with electrospray ionisation tandem mass spectrometry, Rap. Comm. Mass Spec. 19 (2005) 1507–1516.

[44] P. Sikka, J. Sahu, A. Mishra, S. Hashim, Role of aryl urea containing compounds in medicinal chemistry, Med. Chem. 5 (2015) 479–483.

[45] Z. Noorimotlagh, I. Kazeminezhad, N. Jaafarzadeh, M. Ahmadi, Z. Ramezani, S. S. Martinez, The visible-light photodegradation of nonylphenol in the presence of carbon-doped TiO_2 with rutile/anatase ratio coated on GAC: Effect of parameters and degradation mechanism, J. Hazard. Mat. 350 (2018) 108 – 120.